TRANSPORT
2010
25(3): 278–286

VEHICLE GEARBOX DYNAMICS: CENTRE DISTANCE INFLUENCE ON MESH STIFFNESS AND SPUR GEAR DYNAMICS

Viktor Skrickij[1], Marijonas Bogdevičius[2]

Dept of Transport Technological Equipment, Vilnius Gediminas Technical University,
Plytinės g. 27, LT-10105 Vilnius, Lithuania
E-mails: [1]skrickij@gmail.com, [2]marius@vgtu.lt

Received 7 March 2010; accepted 19 July 2010

Abstract. Vehicle gearbox dynamics is characterized by time varying mesh stiffness. The paper presents a survey of methods used for determining mesh stiffness and the analysis of the centre distance influence on it. The refined mathematical transmission model presenting the centre distance as a variable is presented. The centre distance error as well as backlash and bearing flexibility is defined and the influence of these factors on mesh stiffness and spur gear dynamics is investigated. The results obtained from this paper may be used in gear-box diagnostics.

Keywords: vehicle gearbox, spur gear, mesh stiffness, centre distance, dynamics, diagnostic.

1. Introduction

Gear trains are widely used in various means of transport, including air, rail and road transport. One can hardly imagine a modern car, truck or building equipment without switch-gears and gearboxes (Fig. 1), which are used for transmitting torque, speed and direction of rotation. The operating conditions of gears are very complicated because they are subject to torque and dynamic loads due to the anti-torque moment. In the course of operation, some damages are done to gears, which cause vibrations. The analysis of the vibration processes yields the information about the state of gears. There are quite a few methods of data processing obtained from diagnostics. They include the analysis of spectrum, cepstrum, etc. Their survey is beyond the aims of the present paper, therefore, the works of Balickij *et al.* (Балицкий *и др*. 1984), Staszewski and Worden (1997), Mažeika (2008) may be recommended for getting into more details. The methods stated above are used as a tool of data processing. Effective diagnostics require precise data about particular defects and their influence on the considered mechanism. In addition, the frequency at which a certain defect can be observed and the dependence of its development on the amplitude of the signal should be known. To obtain these data, a lot of expensive and time-consuming experiments should be made. Therefore, mathematical modelling may be effectively used for this purpose.

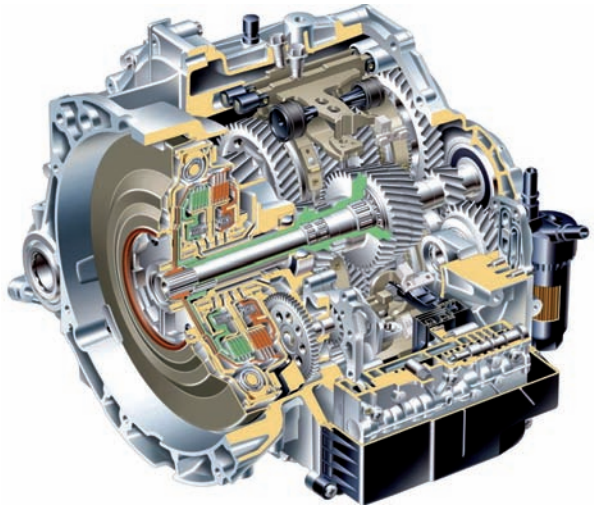

Fig. 1. Gearbox

Gear trains are deliberated to be the investigation object of many research works. Thus, the work of Utagawa (1958) is aimed at determining the dynamic loads. Time-varying stiffness is considered as well. The equations for calculating the dynamic loads are given and all theoretical calculations are checked by practical experiments. The research of Augustaitis (Аугустайтис 1994) is worth paying attention because the Bulgakov's system of normal coordinate is used and mathematical models of gear trains, bearings and shafts are presented. Ragulskis *et al.* (Рагульскис *и др*. 1974) investigated friction in bearings as well as their stiffness and lateral vibration and performed the ex-

perimental research into bearings. Mariūnas (Марюнас 1993) analyzed kinematic gear trains with force closure of links. Mathematical models are being constantly improved and new models are being constructed. Multistage gear systems are being investigated now. Thus, Fakhfakh *et al.* (2006) uses a mathematical model to describe a two-stage gear system and step function to describe stiffness. Litak and Friswell (2005) consider gear defects, i. e. tooth breaks, pitch errors, etc., applying the chaos theory. Gill-Jeong (2007) presented a mathematical model of two-stage gear systems and Fourier series which are used for describing stiffness. In addition, backlash is determined and damping coefficient is calculated. The formulas for determining the combined torsional mesh stiffness of one and two spur gear pairs in mesh are offered by Kiekbusch and Howard (2007). It is assumed that the total stiffness consists of gear stiffness, tooth stiffness and contact stiffness of gears. Walha *et al.* (2009), discusses bearing flexibility and backlash of both gears. Stiffness variation is described by step function. Frolov and Kosarev (2003) analyse the factors, influencing the vibration processes, e.g. mesh stiffness, forces, pitch errors, profile errors, etc. Zouari *et al.* (2007) studies the effect of cracking on mesh stiffness. They varied in crack size and direction of cracking and were used Finite Element Method (FEM) for calculation. Maliha *et al.* (2004) presented the model of gear-shaft-disk-bearing systems and evaluated the backlash. He *et al.* (2008) presented five models of describing friction. Barzdaitis *et al.* (2006) described a rotating system with gear-wheel coupling and determined the effect of friction on fretting corrosion. The problem was solved by FEM. Mažeika *et al.* (2008) investigated gear train with antifriction bearings. FEM was also used for calculation. The aim of the paper was to suggest some methods for protecting the systems with gear power transmission, running on antifriction bearings, from unexpected failures. Barzdaitis *et al.* (2009) analysed the problem connected with the increased loading of bearings, when the mechanism was being turned off. Displacements and kinematic orbits were used as a diagnostic tool.

2. Methods of Determining Mesh Stiffness in a Pair of Teeth

In this section, a survey of methods for determining mesh stiffness, which may be used in constructing a mathematical model, is presented.

2.1. Model 1

Using a method suggested by Dimentberg and Kolesnikov (Диментберг и Колесников 1980) and changing it so that stiffness dimension is [N/m], we get the following expression (Fig. 2):

$$k = \frac{E \cdot b}{11.2 + 7.5 \cdot (h - 1.25)^2}, \quad (1)$$

where: E is reduced Young's modulus; b is width of the teeth, while the numerical values are available in Table; h is a relative distance from the point of load application to the tooth base, ranging from 0.25 to 2.25.

Table. A mathematical model data

Parameter	Value
Young's modulus, E	210.0 GPa
Module, m	$2.500 \cdot 10^{-3}$ m
Number of teeth, pinion, z_1	30
Number of teeth, gear, z_2	30
Tooth width, b	$1.000 \cdot 10^{-2}$ m
Motor parameter, c_v	147.4
Motor parameter, d_v	34.48
Angular velocity of idle running, ω_0	157.1 rad/s
Moment of inertia, engine, I_1	$5.400 \cdot 10^{-3}$ kg·m^2
Reduced moment of inertia, pinion, I_2	$9.620 \cdot 10^{-3}$ kg·m^2
Reduced moment of inertia, gear, I_3	$9.620 \cdot 10^{-3}$ kg·m^2
Moment of inertia, load, I_4	$5.400 \cdot 10^{-3}$ kg·m^2
Reduced mass of pinion, m_1	1.660 kg
Reduced mass of gear, m_2	1.660 kg
Torsional stiffness coefficient of rotor, k_r	$30.66 \cdot 10^3$ Nm/rad
Torsional damping coefficient of rotor, c_r	100.0 N·m/s
Reduced bearing stiffness coefficient, k_b	$1.000 \cdot 10^8$ N/m
Reduced bearing damping coefficient, c_b	1000 N·s/m
Mesh damping coefficient, c	100.0 N·s/m
Density, ρ	7800 kg/m^3
Speed recovery factor, e_n	0.7000
Coefficient, a_b	1.500
Profile angle, α_0	0.3490 rad
Pressure angle, α_w	0.3490 rad
Orientation angle, ψ	0 rad
Reduced Young's modulus, E_b	115.4 GPa

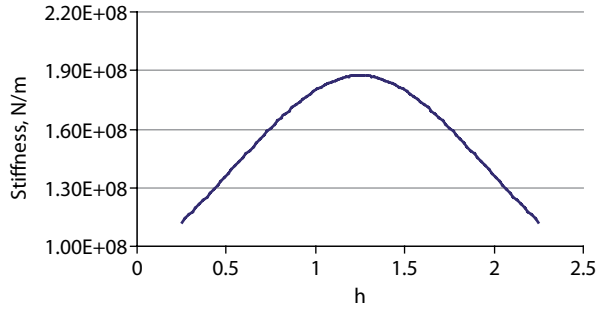

Fig. 2. Model 1: Stiffness dependence on the parameter h

To go over from the parameter h to contact ratio, the following expression should be used:

$$k = \frac{E \cdot b}{11.2} \cdot \left(1 - 0.4 \cdot \left(1 - \frac{2 \cdot X}{\varepsilon}\right)^2\right), \quad (2)$$

where: ε is the contact ratio; X is a variable and $X \in [0; \varepsilon]$.

2.2. Model 2

It was suggested by Dimentberg and Kolesnikov (Диментберг и Колесников 1980). When this method

is used for calculation, the character of the curve remains the same as in the previous case, but stiffness is different and formula is changed so that the stiffness dimension is [N/m]. The total stiffness of a teeth pair may be found as follows (Fig. 3):

$$k = \frac{E \cdot b}{13} \cdot \left(1 - 0.27 \cdot \left(h - 1.25\right)^2\right), \quad (3)$$

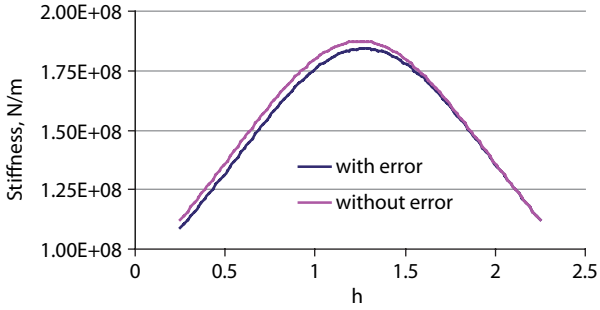

Fig. 3. Model 2: Stiffness dependence on the parameter *h*

2.3. Model 3

Model 3 allows us to determine the variation of the centre distance (Дименберг и Колесников 1980):

$$k = \frac{E \cdot b}{3.65 + h^3 + 3.65 + \left(k_d - h\right)^3}, \quad (4)$$

where:

$$k_d = 2.5 + \frac{\Delta A}{m}, \quad (5)$$

where: $\Delta A = 0.1$ mm is the centre distance error; m is the module.

The main disadvantage of this method is that only stiffness is changed, while the meshing area has not changed (Fig. 4).

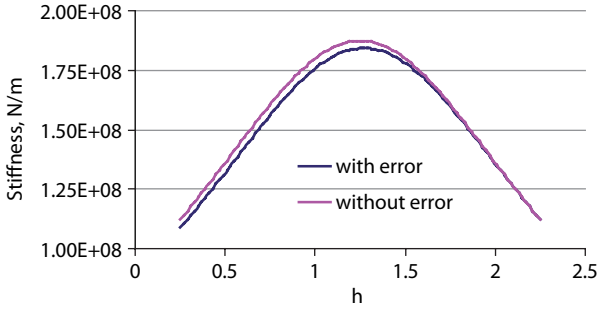

Fig. 4. Model 3: Stiffness with and without centre distance error

2.4. Model 4

Kuang and Yang offered a method for determining stiffness of one tooth, Kuang and Yang (1992), Kuang and Lin (2001). Using this method, we obtain the stiffness of one tooth:

$$K_i\left(r\right) = \left(A_0 + A_1 \cdot X_i\right) + \left(A_2 + A_3 \cdot X_i\right) \frac{r - r_{wi}}{\left(1 + X_i\right) \cdot m}; \quad (6)$$

$$A_0 = 3.867 + 1.612 \cdot z_i - 0.02916 \cdot z_i^2 + 0.0001553 \cdot z_i^3; \quad (7)$$

$$A_1 = 17.060 + 0.7289 \cdot z_i - 0.01728 \cdot z_i^2 + 0.0000999 \cdot z_i^3; \quad (8)$$

$$A_2 = 2.637 - 1.222 \cdot z_i + 0.02217 \cdot z_i^2 - 0.0001179 \cdot z_i^3; \quad (9)$$

$$A_3 = -6.330 - 1.033 \cdot z_i + 0.02068 \cdot z_i^2 - 0.0001130 \cdot z_i^3, \quad (10)$$

where: $i = 1.2; r$ is the radius at loading point; z_i is the number of teeth; X_i is addendum modification; $X_i = 0; r_{wi}$ is pitch radius. When stiffness dimension is [N/m]:

$$k_i = K_i\left(r\right) \cdot b \cdot 10^9, \quad (11)$$

when the stiffness of both gears is determined, the total mesh stiffness is found as follows:

$$K = \frac{k_1 \cdot k_2}{k_1 + k_2}. \quad (12)$$

Using this method, centre distance variation may be determined. Given the stiffness at any point of the tooth, the matching points of two teeth are determined by centre distance.

As one can see, unlike the situation in Model 3, the area of load application also changed (Fig. 5).

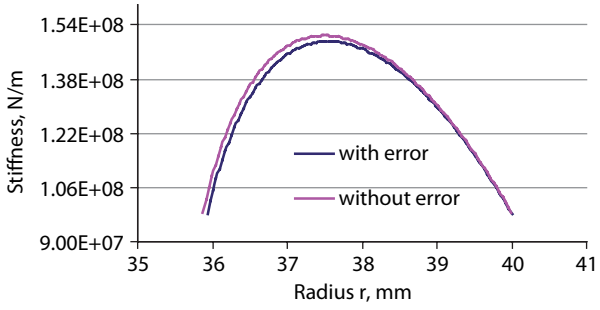

Fig. 5. Model 4: Stiffness with and without centre distance error (ΔA = 0.1 mm)

2.5. Model 5

Stiffness can be calculated by using FEM.

The beam element with four degrees of freedom is used, and only a bending force is evaluated. Given longitudinal stiffness distribution, we may get stiffness dependence on the rotation angle of the gear (Fig. 6).

2.6. Model 6

This is an analytical method. If only bending is calculated, while compression is not considered, the displacement is determined as follows:

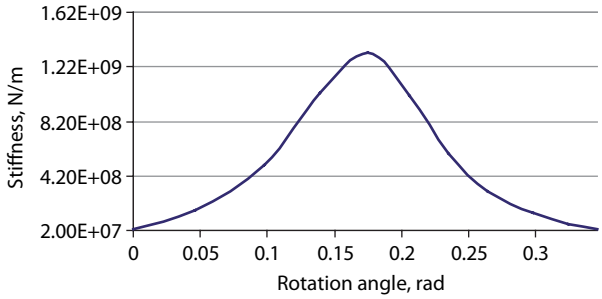

Fig. 6. Model 5: Stiffness dependence on the rotation angle

$$q_i = \frac{\partial U}{\partial F} = \frac{\partial}{\partial F}\left(\int_{x_i} \frac{M_{x_i}^2 dx}{2EI_{x_i}}\right) = \int_{x_i} \frac{M_{x_i} dx}{EI_{x_i}} \cdot \frac{\partial M_{x_i}}{\partial F}, \quad (13)$$

where: U is the potential energy; F is a force; M_{x_i} is a gear torque; I_{x_i} is the inertia moment of tooth cross section.

Rearranging the expression (13), we get:

$$q_i = \int_0^{x_i} \frac{-Fx_i dx_i}{EI_{x_i}} \cdot \left(-x_i\right) = \frac{Fx_i^3}{3EI_{x_i}}. \quad (14)$$

The stiffness of the gear tooth is obtained this way:

$$k_i = \frac{F}{q_i} = \frac{3EI_{x_i}}{x_i^3}, \quad (15)$$

where: x_i is a distance from the tooth base to the area of force application. Mesh stiffness in a pair of gears is determined by the formula (12) (Fig. 7).

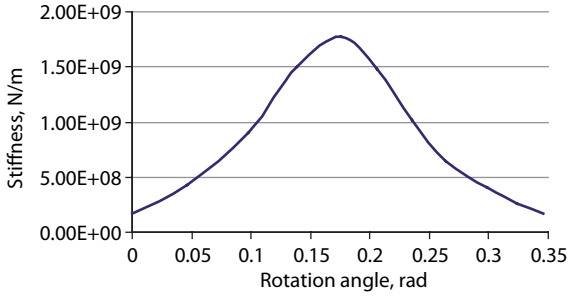

Fig. 7. Model 6: The dependence of stiffness on the rotation angle

The compression strength of the tooth may also be determined. Taking into account bending, the calculations, compression and contact stiffness were made by Atanasiu and Doroftei (2008).

We have analysed six models of gear meshing in order to determinate the mesh stiffness. Models 3, 4, 5 and 6 allow us to evaluate the variation of the centre distance. However, when model 3 is used, the point, where interaction between the teeth begins, does not change. In further calculations, the method of determining mesh stiffness offered by Kuang and Yang (1992) is used.

3. A Mathematical Transmission Model with an Asynchronous Electric Motor

A mathematical model of transmission is considered (Fig. 8). In Fig. 8, 1 is an asynchronous electric motor. Its main parameters are the moment of inertia I_1 and the rotation angle φ_1. The numbers 2, 3, 4, 5 denote bearings with the reduced stiffness coefficient k_b and the reduced damping coefficient c_b. 6, 7 denote the pinion and gear, having the reduced moments of inertia I_2, I_3, the reduced masses m_1, m_2 and the rotation angles φ_2, φ_3. 8 means the load with the moment of inertia I_4, the rotation angle φ_4 and the load moment M_4.

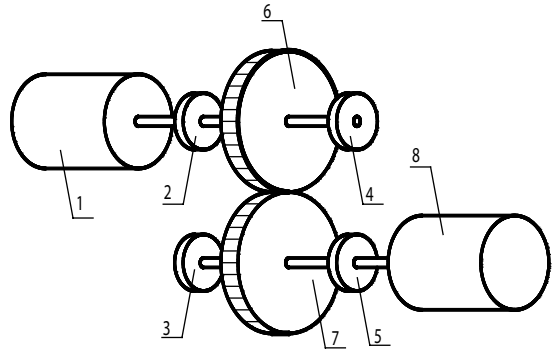

Fig. 8. A schematic view of transmission: 1 – electric motor; 2, 3, 4, 5 – bearings; 6, 7 – pinion and gear; 8 – load

3.1. A Mathematical Model of an Asynchronous Electric Motor

To evaluate the non-uniformity rotation of the transmission elements, a mathematical model suggested by Bogdevičius (2008) may be used:

$$\dot{M}_1 + d_v \cdot M_1 = c_v \cdot \left(\omega_0 - \dot{\varphi}_1\right), \quad (16)$$

where: M_1 is the rotation moment of the electric motor; d_v, c_v are the parameters of the electric motor; ω_0 is an angular velocity of idle running; $\dot{\varphi}_1$ is an angular velocity of electric motor.

3.2. A Mathematical Model of Rotary Motion Transmission

The dynamic of gearing is described by equations:

$$I_1 \cdot \ddot{\varphi}_1 = M_1 - k_r \cdot \left(\varphi_1 - \varphi_2\right) - c_r \cdot \left(\dot{\varphi}_1 - \dot{\varphi}_2\right); \quad (17)$$

$$I_2 \cdot \ddot{\varphi}_2 = k_r \cdot \left(\varphi_1 - \varphi_2\right) + c_r \cdot \left(\dot{\varphi}_1 - \dot{\varphi}_2\right) - M_2; \quad (18)$$

$$M_2 = F \cdot r'_{w1}; \quad (19)$$

$$I_3 \cdot \ddot{\varphi}_3 = M_3 - k_r \cdot \left(\varphi_3 - \varphi_4\right) - c_r \cdot \left(\dot{\varphi}_3 - \dot{\varphi}_4\right); \quad (20)$$

$$M_3 = -F \cdot r'_{w2}; \quad (21)$$

$$I_4 \cdot \ddot{\varphi}_4 = k_r \cdot \left(\varphi_3 - \varphi_4\right) + c_r \cdot \left(\dot{\varphi}_3 - \dot{\varphi}_4\right) - M_4, \quad (22)$$

where: k_r, c_r are torsional rotor stiffness and damping coefficients; M_2, M_3 are moments; F is meshing force, r'_{w1}, r'_{w2} are variable pitch radii.

3.3. A Model of Meshing of a Pair of Gears

Force F and variable radii r'_{w1}, r'_{w2} were described above. However, nothing was said about their calculation. In this section, geometrical calculation of centre distance, varying in time is presented, and the forces found in bearings and meshes are determined. All calculations are made using the model presented in Fig. 9. Bearing flexibility is characterized by a backlash: δ_b, δ_0 denote a backlash; ψ_1 is an orientation angle used to determine gear train location on the plane; α_{w1} is a pressure angle.

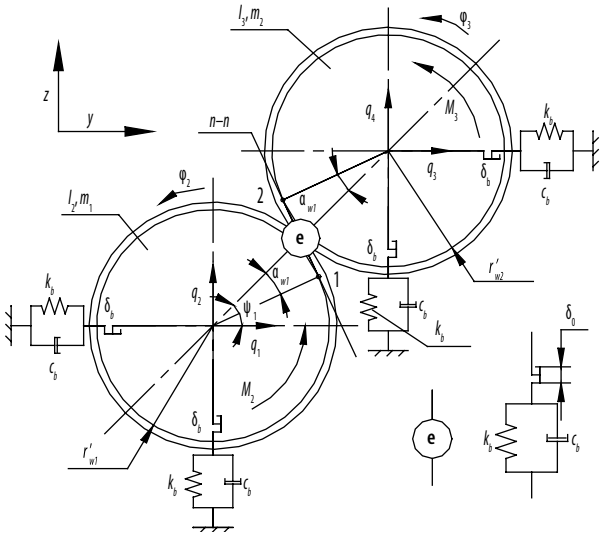

Fig. 9. Gear mesh

The centres of gears are moving because they are subject to rotation moments (M_2, M_3). To determinate their location at any moment of time the displacement vectors q_1, q_2, q_3, q_4 are used.

Errors may occur in manufacturing gear parts. When parts are being assembled into units, the number of errors increases. With the increase of the service life of the mechanism, the number of faults is increasing, while backlashes are getting wider and flexibility of units is growing. Developing a mathematical model of gear train, the variation of the centre distance should be evaluated.

The centre distance depends on the accuracy of manufacturing. However, a certain deviation from the nominal size is inevitable. When a gear train is loaded, gears are displaced with respect to each other, causing further variation of centre distance. In the operating mode of the mechanism, bearing flexibility is growing, causing further changing of the centre distance. For example, if the initial centre distance is a, in an operating gear train, it is equal to a_1.

Centre distance consists of the nominal (design) centre distance a_0 and the geometric error ΔA:

$$a = a_0 + \Delta A. \tag{23}$$

Under the action of the force F, gear wheels are displaced with respect to each other, and centre distance a_1 is obtained. Centre distance a_1 is calculated as follows (Fig. 10):

$$a_{1y} = a_y - q_1 + q_3; \tag{24}$$

$$a_{1z} = a_z - q_2 + q_4, \tag{25}$$

where:

$$a_y = a \cdot \cos\psi; \tag{26}$$

$$a_z = a \cdot \sin\psi; \tag{27}$$

ψ is an initial orientation angle;

$$a_1 = \sqrt{a_{1y}^2 + a_{1z}^2}. \tag{28}$$

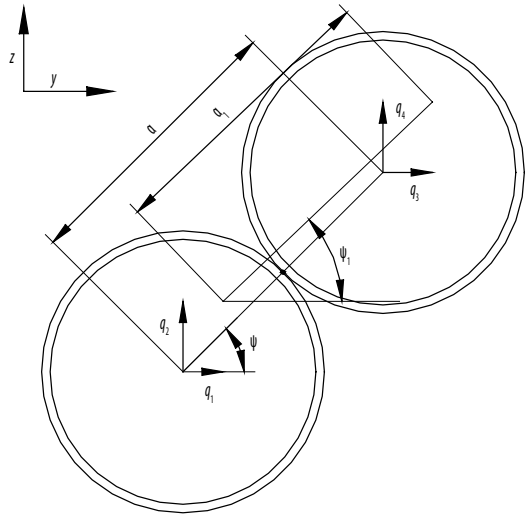

Fig. 10. Centre distance of operating gear train

Calculation of an angle ψ_1 (Fig. 10):

$$\psi_1 = \arccos\frac{a_{1y}}{a_1}. \tag{29}$$

When the centre distance is changed, the original pitch diameter and a pressure angle α_w are also changed. The pressure angle is calculated by the following formula, taking into account the variation of the centre distance:

$$\alpha_{w1} = \arccos\frac{D_{b1} + D_{b2}}{2a_1}, \tag{30}$$

where: D_{bi} is the main gear circle (i = 1, 2). The radii of the changed pitch circles are obtained as follows:

$$r'_{wi} = \frac{D_{bi}}{2 \cdot \cos\alpha_{wi}}. \tag{31}$$

Since q_i is changing in time, the parameters a_1, α_{w1}, ψ_1, r'_{wi} are also varying in time.

The displacements of points 1 and 2 along a straight line which is a tangent line to the circles of both gears (Fig. 9) are calculated as follows:

$$u_1 = r'_{w1} \cdot \varphi_2 - q_1 \cdot \sin\left(\psi_1 - \alpha_{w1}\right) + q_2 \cdot \cos\left(\psi_1 - \alpha_{w1}\right); \quad (32)$$

$$u_2 = r'_{w2} \cdot \varphi_3 - q_3 \cdot \sin\left(\psi_1 - \alpha_{w1}\right) + q_4 \cdot \cos\left(\psi_1 - \alpha_{w1}\right); \quad (33)$$

$$\delta = u_2 - u_1. \quad (34)$$

The displacement rates of points 1, 2 (Fig. 9) are as follows:

$$\dot{u}_1 = r'_{w1} \cdot \dot{\varphi}_2 - \dot{q}_1 \cdot \sin\left(\psi_1 - \alpha_{w1}\right) + \dot{q}_2 \cdot \cos\left(\psi_1 - \alpha_{w1}\right); \quad (35)$$

$$\dot{u}_2 = -r'_{w2} \cdot \dot{\varphi}_3 - \dot{q}_3 \cdot \sin\left(\psi_1 - \alpha_{w1}\right) + \dot{q}_4 \cdot \cos\left(\psi_1 - \alpha_{w1}\right); \quad (36)$$

$$\dot{\delta} = \dot{u}_2 - \dot{u}_1. \quad (37)$$

The force acting on the mesh is obtained from the expression:

$$F = -k \cdot \delta' - c \cdot \dot{\delta}', \quad (38)$$

where: c is damping coefficient (Fig. 9); k is mesh stiffness determined by the method offered by Kuang and Yang. It should be noted that the parameter r_{wi} = const is used in formula (6).

The influence on the backlash is determined this way:

$$\delta' = \begin{cases} \delta - \delta_0, & \text{if } \delta > \delta_0; \\ 0, & \text{if } \delta_0 \le \delta \le \delta_0; \\ \delta + \delta_0, & \text{if } \delta < -\delta_0. \end{cases} \quad (39)$$

The bearing force is found to be as the following equation:

$$F_{bi} = -k_b \cdot q_i^{1,5} \left(1 + a_b \cdot \left(1 - e_n^2\right) \cdot \frac{\dot{q}_i}{\dot{\Delta}}\right), \quad (40)$$

where: $i = 1, 2, 3, 4$.

The rate of penetration is determined by the formula:

$$\dot{\Delta} = 10^{-5} \sqrt{\frac{E_b}{\rho}}, \quad (41)$$

where: E_b is reduced Young's modulus; ρ is the material density; a_b is a coefficient; e_n is the coefficient of speed recovery.

Axial displacements of gears are determined as follows:

$$m_1 \cdot \ddot{q}_1 = F \cdot \sin\left(\psi_1 - \alpha_{w1}\right) + F_{b1}; \quad (42)$$

$$m_1 \cdot \ddot{q}_2 = -F \cdot \cos\left(\psi_1 - \alpha_{w1}\right) + F_{b2} - m_1 \cdot g; \quad (43)$$

$$m_2 \cdot \ddot{q}_3 = -F \cdot \sin\left(\psi_1 - \alpha_{w1}\right) + F_{b3}; \quad (44)$$

$$m_2 \cdot \ddot{q}_4 = F \cdot \cos\left(\psi_1 - \alpha_{w1}\right) + F_{b4} - m_2 \cdot g, \quad (45)$$

where: g is gravity acceleration.

4. Numerical results and discussion

The initial data presented in Table are used for calculations.

The calculations of mesh stiffness, taking into account the faults of the system, were made.

The graph in Fig. 11 shows the variation of mesh stiffness in time, when centre distance error is $\Delta A = 0;\ 50;\ 100\ \mu m$.

When the error is getting bigger, mesh stiffness and contact ratio are decreasing.

When the backlash is $\delta_0 = 25\ \mu m$ and centre distance errors – $\Delta A = 0;\ 50;\ 100\ \mu m$ – mesh stiffness does not change (Fig. 12). Therefore, it may be stated that, when the motion is steady and the load moment is constant, the backlash does not considerably affect mesh stiffness.

In Fig. 13, the calculation of mesh stiffness with bearing flexibility $\delta_b = 25\ \mu m$ is presented, also the errors of centre distance being $\Delta A = 0;\ 50;\ 100\ \mu m$, respectively. As shown in Fig. 13, mesh stiffness and contact ratio have decreased considerably.

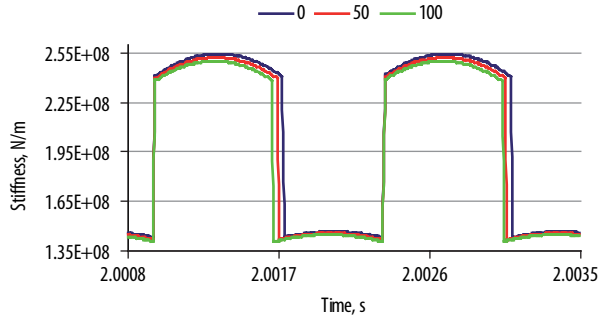

Fig. 11. The influence of the centre distance error on mesh stiffness

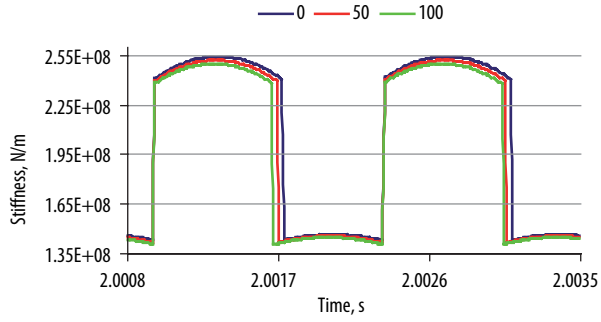

Fig. 12. The influence of the centre distance error and backlash on mesh stiffness

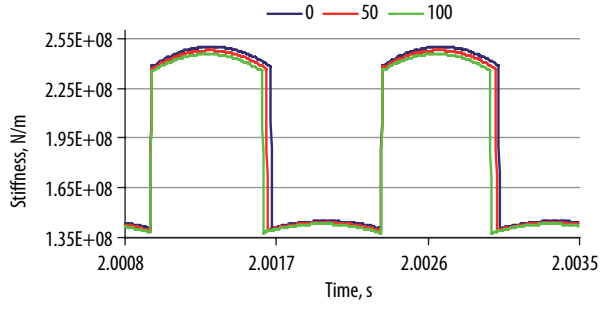

Fig. 13. The influence of the centre distance error and bearing flexibility on mesh stiffness

The damages which influence both the mesh stiffness and the contact ratio are depicted in Figs 11 and 13. Theoretically, the contact ratio of the considered gear train is $\varepsilon = 1.655$, though when lateral displacements are taken into account, its value changes, when the motion is steady (t = 2 s), $\varepsilon = 1.559$, the centre distance error (ΔA = 50 μm) and the contact ratio is equal to ε = 1.539.

When bearing flexibility δ_b = 50 μm is evaluated, the contact ratio is $\varepsilon = 1.519$. When the centre distance error is combined with bearing flexibility, then, the contact ratio is $\varepsilon = 1.500$.

In Fig. 14, the pinion rate spectrum in z direction (Fig. 9) is given for the situation, when no faults are found in the considered gear and the load moment is constant. Six harmonics can be found in the spectrum, matching the gear tooth frequency:

$$f_n = n \cdot f_{rot} \cdot z_i, \tag{46}$$

where: f_{rot} = 24.46 Hz is frequency of rotation; n is the number of harmonic $n = 1, .., 6$.

When centre distance error ΔA = 50 μm is regarded, the numerical values of the considered amplitudes change (Fig. 15). The pinion rate spectrum in z direction, with bearing flexibility is accounted for and given in Fig. 16. The pinion rate spectrum in z direction, with the error of centre distance ΔA = 50 μm and bearing flexibility δ_b = 50 μm are shown in Fig. 17. As shown in Figs 14 and 17, there is the following dependence: when odd harmonics are growing, even harmonics are decreasing.

Though the first harmonic is growing, the increase is very small. It follows from Figs 14 and 17 that the 2-nd harmonic has decreased more than others (76.15%, frequency f_2 = 1468 Hz), while the 5-th harmonic has increased more than others (72.81%, frequency f_5 = 3670 Hz).

The spectrum of the pinion rate in z direction is shown in Figs 18–21 for variable load moment of the considered gear.

Fig. 18 presents the pinion rate spectrum in z direction for the gear having no faults. When centre distance ΔA = 50 μm error was taken into account, the numerical values of the considered amplitudes changed (Fig. 19).

The pinion rate spectrum in z direction with bearing flexibility is shown in Fig. 20.

In Fig. 21, the pinion rate spectrum in z direction is given, with the centre distance error ΔA = 50 μm and bearing flexibility δ_b = 50 μm is taken into account.

The comparison of the results, obtained for constant and variable load moments, shows the same trend of harmonics variation: odd harmonics are increasing, while even harmonics are decreasing.

As shown in Figs 18 and 21, the highest decrease can be observed in the 2-nd harmonic (78.35%, frequency f_2 = 1468 Hz) and in the 5-th harmonic (71.44%, frequency f_5 = 3670 Hz).

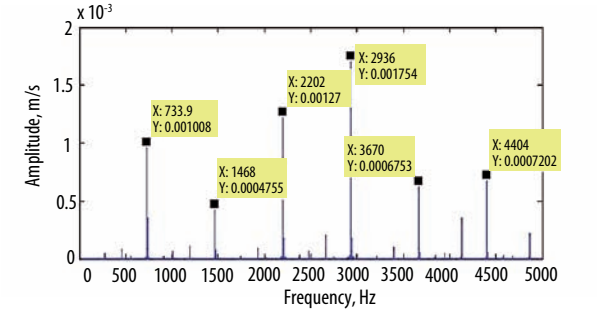

Fig. 14. Spectrum of $\dot{q}_2$, gear without defects, moment $M = M_4$

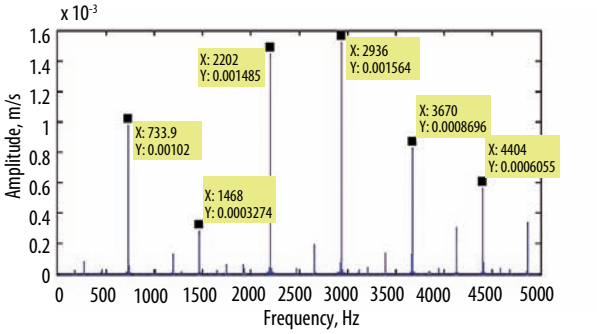

Fig. 15. Spectrum of $\dot{q}_2$, gear with centre distance error ΔA = 50 μm, moment $M = M_4$

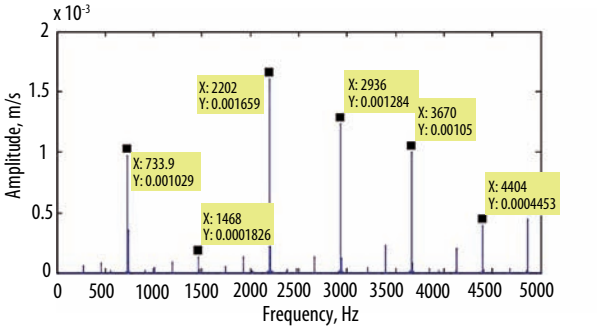

Fig. 16. Spectrum of $\dot{q}_2$, gear with bearing flexibility δ_b = 50 μm, moment $M = M_4$

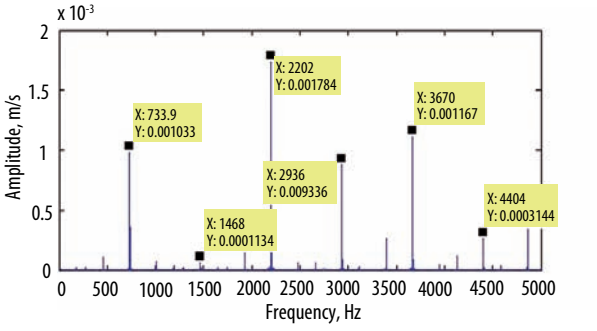

Fig. 17. Spectrum of $\dot{q}_2$, gear with defects ΔA = 50 μm, δ_b = 50 μm, moment $M = M_4$

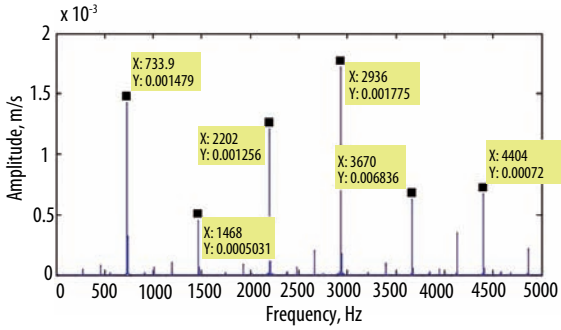

Fig. 18. Spectrum of $\dot{q}_2$, gear without defects, moment $M = M_4 + 0.2 \cdot M_4 \cdot \sin(f_1 \cdot 2 \cdot \pi \cdot t)$

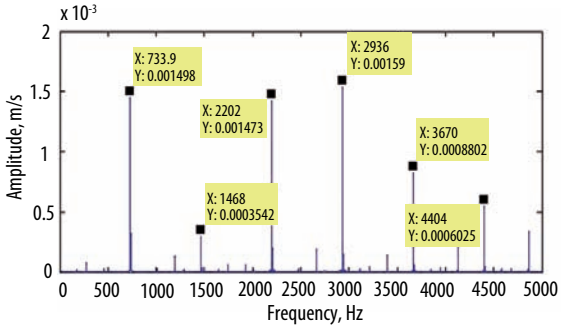

Fig. 19. Spectrum of $\dot{q}_2$, gear with centre distance error ΔA = 50 μ*m*, moment $M = M_4 + 0.2 \cdot M_4 \cdot \sin(f_1 \cdot 2 \cdot \pi \cdot t)$

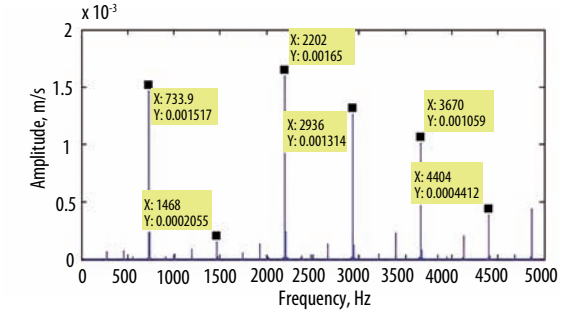

Fig. 20. Spectrum of $\dot{q}_2$, gear with bearing flexibility δ_b = 50 μ*m*, moment $M = M_4 + 0.2 \cdot M_4 \cdot \sin(f_1 \cdot 2 \cdot \pi \cdot t)$

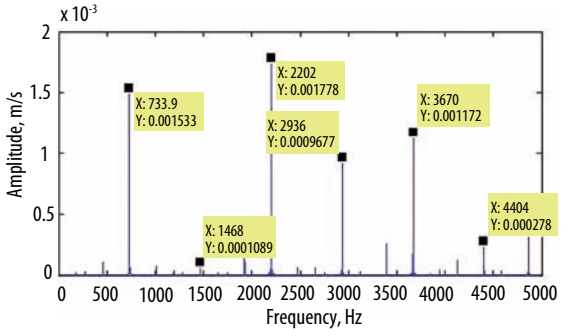

Fig. 21. Spectrum of $\dot{q}_2$, gear with defects ΔA = 50 μ*m*, δ_b = 50 μ*m*, moment $M = M_4 + 0.2 \cdot M_4 \cdot \sin(f_1 \cdot 2 \cdot \pi \cdot t)$

5. Conclusions

1. A refined mathematical transmission model with a variable centre distance is developed. The backlash and bearing flexibility are evaluated.
2. It is determined that, when the motion is steady, the effect of backlash on mesh stiffness is negligible. The analysis of gear rate spectrum shows that, when defects are introduced into gear mesh model, the harmonic amplitudes change. In particular, odd harmonics are increasing, while even harmonics are decreasing. It should be noted that the 1-st harmonic is slightly increasing. The comparison of gear rate spectra given in Fig. 14 and Fig. 17, when the load moment is constant and gear train has (ΔA = 50 μ*m*, δ_b = 50 μ*m*) or does not have defects, shows the highest decrease of the 2-nd harmonic (76.15%, frequency f_2 = 1468 Hz) and the highest decrease of the 5-th harmonic (72.81%, frequency f_5 = 3670 Hz).
3. It is found that centre distance error and bearing flexibility affect mesh stiffness. The larger the amount of errors, the lower mesh stiffness effect is on the variation of contact ratio. Lateral gear displacements affect the variation of contact ratio mostly. Taking into account the effect of displacements, the contact ratio ranges from $\varepsilon = 1.655$ to $\varepsilon = 1.559$ when (t=2 s). When centre distance error ΔA = 50 μ*m* and lateral displacements are considered, contact ratio is equal to $\varepsilon = 1.539$. When bearing flexibility δ_b = 50 μ*m* is also taken into account, contact ratio is reduced to $\varepsilon = 1.500$.

References

Atanasiu, V.; Doroftei, I. 2008. Dynamic contact loads of spur gear pairs with addendum modifications, *European Journal of Mechanical and Environmental Engineering* Fall: 21–26.

Barzdaitis, V.; Bogdevičius, M.; Didžiokas, R. 2006. Dynamic processes of rotating system with coupling, *Solid State Phenomena* 113: 213–218. doi:10.4028/www.scientific.net/SSP.113.213

Barzdaitis, V.; Bogdevičius, M.; Didžiokas, R.; Vasylius, M. 2009. Modeling and diagnostics of gyroscopic rotor, *Journal of Vibroengineering* 11(4): 627–635.

Bogdevičius, M. 2008. *Mechatroninių sistemų ir elementų modeliavimas* [Modelling of mechatronic systems and their elements]. Vilnius: VPU leidykla. 265 p. (in Lithuanian).

Fakhfakh, T.; Walha, L.; Louati, J.; Haddar, M. 2006. Effect of manufacturing and assembly defects on two-stage gear system vibration, *The International Journal of Advanced Manufacturing Technology* 29(9–10): 1008–1018. doi:10.1007/s00170-005-2602-4

Frolov, K. V.; Kosarev, O. I. 2003. Control of gear vibrations at their source, *International Applied Mechanics* 39(1): 49–55. doi:10.1023/A:1023612015873

Gill-Jeong, C. 2007. Nonlinear behavior analysis of spur gear pairs with a one-way clutch, *Journal of Sound and Vibration* 301(3–5): 760–776. doi:10.1016/j.jsv.2006.10.040

He, S.; Cho, S. M.; Singh, R. 2008. Prediction of dynamic friction forces in spur gears using alternate sliding friction formulations, *Journal of Sound and Vibration* 309(3–5): 843–851. doi:10.1016/j.jsv.2007.06.077

Kiekbusch, T.; Howard, I. 2007. A common formula for the combined torsional mesh stiffness of spur gears, in *Proceedings of the 5th Australasian Congress on Applied Mechanics (ACAM 2007),* 10–12 December 2007, Brisbane, Australia, 710–716.

Kuang, J. H.; Lin, A. D. 2001. The effect of tooth wear on the vibration spectrum of a spur gear pair, *Journal of Vibration and Acoustics – Transactions of the ASME* 123(3): 311–317. doi:10.1115/1.1379371

Kuang, J. H.; Yang, Y. T. 1992. An estimate of mesh stiffness and load sharing ratio of a spur gear pair, in *Proceeding of ASME 6th International Power Transmission and Gearing Conference*, 13–16 September 1992, Scottsdale, Arizona, 1–9.

Litak, G.; Friswell, M. I. 2005. Dynamics of a gear system with faults in meshing stiffness, *Nonlinear Dynamics* 41(4): 415–421. doi:10.1007/s11071-005-1398-y

Maliha, R.; Dogruer, C.U.; Özgüven, H. N. 2004. Nonlinear dynamic modeling of gear-shaft-disk-bearing systems using finite elements and describing functions, *Journal of Mechanical Design* 126(3): 534–541. doi:10.1115/1.1711819

Mažeika, P. 2008. *Rotorių su riedėjimo guoliais diagnostikos ir gedimų prevencijos tyrimai:* daktaro disertacija: technologijos mokslai, mechanikos inžinerija (09 T) [Diagnostics and failures prevention researches of rotors with rolling element bearings: Summary of doctoral dissertation: Technological sciences, Mechanical engineering (09 T)]. Kaunas: Technologija. 130 p. (in Lithuanian).

Mažeika, P.; Didžiokas, R.; Barzdaitis, V.; Bogdevičius, M. 2008. Dynamics and reliability of gear driver with antifriction bearings, *Journal of Vibroengineering* 10(2): 217–221.

Staszewski, W. J.; Worden, K. 1997. Classification of faults in gearboxes – pre-processing algorithms and neural networks, *Neural Computing & Applications* 5(3): 160–183. doi:10.1007/BF01413861

Utagawa, M. 1958. Dynamic loads on spur gear teeth, *Bulletin of the JMSE* 1(4): 397–403.

Walha, L.; Fakhfakh, T.; Haddar, M. 2009. Nonlinear dynamics of a two-stage gear system with mesh stiffness fluctuation, bearing flexibility and backlash, *Mechanism and Mashine Theory* 44(5): 1058–1069. doi:10.1016/j.mechmachtheory.2008.05.008

Zouari, S.; Maatar, M.; Fakhfakh, T.; Haddar, M. 2007. Three-dimensional analyses by finite element method of a spur gear: effect of cracks in the teeth foot on the mesh stiffness, *Journal of Failure Analysis and Prevention* 7(6): 475–481. doi:10.1007/s11668-007-9078-5

Аугустайтис, В.-К. 1994. *Анализ и синтез колебаний машин в применении к приводу металлорежущих станков* [Augustaitis, V. K. Analysis and synthesis of vibrations within the machines as applied to the drive units of machine tools]. Вильнюс: Техника. 306 с. (in Russian).

Балицкий, Ф. Я.; Иванова, М. А.; Соколова, А. Г.; Хомяков, Е. И. 1984. *Виброакустическая диагностика зарождающихся дефектов* [Balickij, F. Y.; Ivanova, M. A.; Sokolova, A. G.; Chomyakov, E. I. Vibroacoustic diagnostics of the developing defects]. Москва: Наука. 119 с. (in Russian).

Диментберг, Ф. М.; Колесников, К. С. 1980. *Вибрации в технике*. Том 3. *Колебания машин, конструкций и их элементов* [Dimentberg, F. M.; Kolesnikov, K. S. Vibration in technology, Vol 3. Vibration of machines, structures and their elements]. Москва: Машиностроение. 544 с. (in Russian).

Марюнас, М. 1993. *Кинематические зубчатые передачи с силовым замыканием звеньев*: монография [Mariūnas, M. Kinematic gear trains with force closure of links: Monograph]. Вильнюс: Издательство науки и энциклопедий. 194 с. (in Russian).

Рагульскис, К.; Юркаускас, А.; Атступенас, В.-Р.; Виткуте, А.-Э.; Кульвец, А. 1974. *Вибрации подшипников* [Ragulskis, K.; Jurkauskas, A.; Atstupėnas, V. R.; Vitkutė, A. E.; Kulvets, A. Vibration of bearings]. Вильнюс: Минтис. 391 с. (in Russian).